

Speeding up parallel tempering simulations

Martin Hasenbusch* and Stefan Schaefer†

*Institut für Physik, Humboldt-Universität zu Berlin,
Newtonstr. 15, 12489 Berlin, Germany*

(Dated: October 1, 2018)

Abstract

We discuss methods that allow to increase the step-size in a parallel tempering simulation of statistical models and test them at the example of the three-dimensional Heisenberg spin glass. We find an overall speed-up of about two for contemporary lattices.

PACS numbers: 05.10.Ln, 61.43.Bn, 64.70.kj

arXiv:1006.4247v2 [cond-mat.stat-mech] 19 Oct 2010

* Martin.Hasenbusch@physik.hu-berlin.de

† Stefan.Schaefer@physik.hu-berlin.de

I. INTRODUCTION

The Monte Carlo simulation of statistical models with a rugged free energy landscape is notoriously difficult. At low temperatures the simulation might get stuck in one of the valleys of the free energy, which leads to very large auto-correlation times. One way to overcome this problem is the so called parallel tempering algorithm, also called random exchange method or multiple Markov-chain method [1, 2].

In a parallel tempering simulation, N replicas of the statistical system are simulated in parallel at different temperatures. From the low temperature which is the target of the investigation, a tower of intermediate temperatures is built up to a point, where the configurations can move easily from one valley of the free energy to an other. Let us denote the inverse of these temperatures by $\beta_1 < \beta_2 < \dots < \beta_N$.

The parallel tempering method involves two components. One is the update of each individual replica, independently of the others, using a standard algorithm, e.g. local Metropolis updates. The other are updates that allow to swap two configurations between neighboring temperatures. With this step, configurations can travel from low to high temperatures and back and thereby bypass the barriers at low temperatures.

In most implementations, this is realized by proposing the exchange of the field configurations at inverse temperatures β_i and β_{i+1} . This is accepted with the probability

$$A_{\text{swap}} = \min[1, \exp((\beta_{i+1} - \beta_i)(H_{i+1} - H_i))] , \quad (1)$$

where H_{i+1} and H_i are the values of the Hamiltonian of the replica at β_{i+1} and β_i , respectively. For most systems, this is an inexpensive step, however, if the temperatures are chosen too far apart, the acceptance rate will very quickly drop to zero. Therefore, the β_i have to be chosen close enough such that the acceptance rate $\langle A_{\text{swap}} \rangle \gtrsim 0.1$. In particular for large systems, this can require the use of large numbers of intermediate temperatures, at each of which a replica has to be simulated.

Here we discuss modifications of the replica exchange step of the algorithm. The basic idea is to not simply swap the two replica, but to modify them in such a way as to improve the probability that the move is accepted. These modifications lead to a higher acceptance rate at given differences $\beta_{i+1} - \beta_i$ or the same acceptance rates can be achieved using larger differences in the inverse temperature.

We like to mention that in [3, 4] annealed swapping is used to this end. The authors of [3], who have simulated the two-dimensional XY model on the square lattice, could indeed reach larger steps in the temperature, however, this progress does not compensate for the additional effort needed for the auxiliary update steps. The authors of [4] have performed a molecular dynamics simulation of 10 classical non-interacting particles in a potential with several local minima. They find that annealed swapping “is able to achieve the computational efficiency of ordinary replica exchange, using fewer replicas.”

In this work, we shall discuss these methods for the example of the three-dimensional Heisenberg spin glass, however, they are quite general and can be easily adapted to other models. The Monte Carlo simulation of spin glasses in general is quite challenging. For the three-dimensional Ising spin glass at the transition temperature and at temperatures below, only lattices up to 32^3 have been simulated [5]. While there is consensus that the model undergoes a second order phase transition, the error bars of critical exponents are quite large.

In this letter, we discuss the case of the physically more realistic Heisenberg spin glass, where even the nature of the phase transition is still under debate. Recent works are [6, 7].

We consider the Heisenberg spin glass on a simple cubic lattice with periodic boundary conditions. The classical Hamiltonian is given by

$$H = - \sum_{\langle xy \rangle} J_{xy} \vec{s}_x \cdot \vec{s}_y , \quad (2)$$

where the field variables \vec{s}_x are unit vectors with three real components; x and y denote the sites of the lattice. The summation runs over pairs $\langle xy \rangle$ of nearest neighbor sites. The J_{xy} are nearest neighbor interactions with a Gaussian distribution of zero mean and standard deviation unity. For each set of these quenched interactions, the expectation values of the observables are computed and then averaged over different realizations of the J_{xy} .

II. OBSERVABLES

In order to study the performance of the algorithm, we have measured the overlap susceptibility, which is constructed from the overlap variable

$$q_{\alpha,\beta,x} = s_{\alpha,x}^{(1)} s_{\beta,x}^{(2)} , \quad (3)$$

where $\vec{s}_x^{(1)}$ and $\vec{s}_x^{(2)}$ are the fields at the site x of two statistically independent configurations $\{\vec{s}\}^1$ and $\{\vec{s}\}^2$. The overlap susceptibility is then given by

$$\chi = \frac{1}{L^3} \sum_{\alpha,\beta} \left[\sum_x q_{\alpha,\beta,x} \right]^2 . \quad (4)$$

Furthermore, we have measured the internal energy defined by

$$E = \frac{1}{L^3} \sum_{\langle xy \rangle} J_{xy} \vec{s}_x \cdot \vec{s}_y . \quad (5)$$

In a physics study of the model, one would consider a larger list of quantities, including e.g. the second moment correlation length and various cumulants. Also one might study so called chiral quantities; see Refs. [6, 7] for their definition.

To get the two independent configurations required by Eq. (3), we simulated, as it is usually done, two copies of the system for each of the temperatures. Alternatively one might simulate a single copy and store the configurations on disk. Then one can combine configurations that are separated by $t \gg \tau$ in the Markov chain, where τ is the autocorrelation time.

III. IMPROVED REPLICA EXCHANGE

In the following two sections, we describe two methods, which improve on the traditional replica exchange between neighboring temperatures. The first is a decimation procedure, where we study the update under an effective action in which half the fields have been integrated out. It is described in Sec. III A. In the second procedure, given in Sec. III B, we apply an invertible cooling/heating transformation of the fields, which leads also to a higher acceptance in the exchange step. For completeness, we give the details of the hybrid-overrelaxation algorithm used to simulated the individual replica between the exchange steps in Sec. III C.

A. Decimation

The method described in this section is applicable to general models, where a sub-set of lattice points can be chosen such, that they do not interact among each other. Since the generalization to other models, e.g. the Ising spin glass, is trivial, we stay in our discussion with the Heisenberg spin glass model on the simple cubic lattice. The partition function in terms of the action

$$S[\beta, \{\vec{s}\}] = \beta H[\{\vec{s}\}] = -\beta \sum_{\langle xy \rangle} J_{xy} \vec{s}_x \cdot \vec{s}_y \quad (6)$$

is given by

$$Z = \prod_x \left[\int d\vec{s}_x \right] \exp(-S[\beta, \{\vec{s}\}]) . \quad (7)$$

The simple cubic lattice can be divided into two sub-sets of points, one called white (W), the other black (B), such that the black points have only white neighbors and vice versa. This allows us to write the partition function as

$$Z = \prod_{x \in W} \left[\int d\vec{s}_x \right] \prod_{x \in B} \left[\int d\vec{s}_x \right] \exp(-S[\beta, \{\vec{s}\}]) , \quad (8)$$

where now all the integrations over the fields on the black sites can be performed:

$$\prod_{x \in B} \left[\int d\vec{s}_x \right] \exp(-S[\beta, \{\vec{s}\}]) = \prod_{x \in B} \left[\int d\vec{s}_x \exp(\beta \vec{s}_x \cdot \vec{S}_x) \right] = \prod_{x \in B} I(\beta \vec{S}_x) \quad (9)$$

where

$$\vec{S}_x = \sum_{y.nn.x} J_{xy} \vec{s}_y \quad (10)$$

is the sum over the fields on the nearest neighbor sites of x . In Eq. (9) we have introduced the abbreviation

$$I(\beta \vec{S}_x) = \int d\vec{s}_x \exp(\beta \vec{s}_x \cdot \vec{S}_x) . \quad (11)$$

In the case of the Heisenberg model, this integral can be easily performed

$$\begin{aligned} \int ds_{1,x} \int ds_{2,x} \int ds_{3,x} \delta(\vec{s}_x^2 - 1) \exp(R_x s_{1,x}) &= c \int_{-1}^1 ds_{1,x} \exp(R_x s_{1,x}) \\ &= \frac{2c}{R_x} \sinh(R_x) , \end{aligned} \quad (12)$$

where we have rotated the problem such that \vec{S}_x is a multiple of $(1, 0, 0)$ and $R_x = \beta |\vec{S}_x|$. Putting everything together, the partition function reads

$$Z = \prod_{x \in W} \left[\int d\vec{s}_x \right] \exp(-\tilde{S}[\beta, \{\vec{s}\}_W]) \quad \text{with} \quad \tilde{S}[\beta, \{\vec{s}\}_W] = - \sum_{x \in B} \ln I(\beta \vec{S}_x) , \quad (13)$$

where the subscript W indicates that \tilde{S} depends only on the fields on the white sites.

Now we perform a tempering step with the fields on the white sites only, using the action $\tilde{S}(\beta, \{\vec{s}\}_W)$. Given a field $\{\vec{s}\}_W^1$ at β_1 and a field $\{\vec{s}\}_W^2$ at β_2 , the proposal is to swap to $\{\vec{s}\}_W^2$ at β_1 and $\{\vec{s}\}_W^1$ at β_2 . The acceptance probability for this swap is given by

$$A_{\text{swap}} = \min \left[1, \frac{\prod_{x \in B} I(\beta_2 \vec{S}_x^{(1)}) \prod_{x \in B} I(\beta_1 \vec{S}_x^{(2)})}{\prod_{x \in B} I(\beta_1 \vec{S}_x^{(1)}) \prod_{x \in B} I(\beta_2 \vec{S}_x^{(2)})} \right]. \quad (14)$$

In the case of the Heisenberg model, the evaluation of this expression is relatively simple. First we notice that the prefactors $\frac{2c}{R_x}$ cancel. Therefore it remains to evaluate $\prod_{x \in B} \sinh(R_x)$, for which details are given in Appendix A.

In principle, one could also perform the updates using the decimated action $\tilde{S}(\beta, \{\vec{s}\}_W)$. However there is no efficient update for this action. The best idea might be to perform local Metropolis updates of $\{\vec{s}\}_W$. This would require to evaluate $\Delta \tilde{S}(\beta, \{\vec{s}\}_W)$, which is relatively expensive.

Instead, after the tempering step, we insert the fields on the black sites again, using their (local) Boltzmann weight. Technically, this is done in exactly the same way as a heatbath update is performed. Having restored the fields on the black sites, we can perform overrelaxation and heatbath sweeps as usual.

In our simulations, in order to save CPU-time, we only insert new fields on the black sites if the swap is accepted, otherwise the fields keep their old values. Furthermore, we alternate the role of black and white sites from one pair of β -values to the next. In the case of the first pair, we chose randomly whether the fields on black or white sites are decimated.

B. Cooling and Heating

Let us now turn to the second idea to improve the replica exchange step. Inspired by the field transformations proposed in the framework of the Hybrid Monte Carlo algorithm [8], it improves on the standard step, which exchanges just the configuration $(\{\vec{s}\}^1, \{\vec{s}\}^2) \rightarrow (\{\vec{s}\}^2, \{\vec{s}\}^1)$ evaluating the action at the respective other parameters by applying an invertible field transformation to the configurations

$$(\{\vec{s}\}^1, \{\vec{s}\}^2) \rightarrow (\mathcal{F}(\{\vec{s}\}^2), \mathcal{F}^{-1}(\{\vec{s}\}^1)) .$$

This can be successful, if we manage to find a transformation, which transforms a “typical” configuration from temperature No. 1 into one more like those at temperature No. 2 and vice versa. Obviously this update is reversible. For the acceptance probability one has to take the Jacobian determinant $\det J_{\mathcal{F}}(\cdot)$ of the transformation into account. For a general transformation we can then use the acceptance probability

$$A_{\text{swap}} = \min \left[1, \frac{\det J_{\mathcal{F}}(\{\vec{s}\}^2) \exp \{-\beta_1 H[\mathcal{F}(\{\vec{s}\}^2)] - \beta_2 H[\mathcal{F}^{-1}(\{\vec{s}\}^1)]\}}{\det J_{\mathcal{F}}(\{\vec{s}\}^1) \exp \{-\beta_1 H[\{\vec{s}\}^1] - \beta_2 H[(\{\vec{s}\}^2)]\}} \right]. \quad (15)$$

For most transformations, computing the Jacobian is a very cumbersome task, it is therefore advisable to use a transformation, which is composed of elementary steps f , which only manipulate one field variable at a time and only depend on its nearest neighbors. Then the Jacobian matrix $\partial s' / \partial s$, where $s' = f(s)$, can be easily computed along with its determinant.

For the Heisenberg spin glass, we propose a transformation which is cooling the configuration when moving towards a lower temperature and heating it up when moving towards a higher one. The specific f we tested here is given by

$$\vec{s}'_x = \vec{s}_x \cos \alpha + \frac{\vec{p}}{|\vec{p}|} \sin \alpha$$

with $\alpha = \epsilon |\vec{p}|$ where ϵ is a tunable parameter. \vec{p} is the vector in the \vec{s}_x - \vec{S}_x plane orthogonal to \vec{s}_x

$$\vec{p} = \vec{S}_x - (\vec{S}_x \cdot \vec{s}_x) \vec{s}_x$$

with \vec{S}_x as defined in Eq. (10). In case of cooling, it reduces the angle between the \vec{S}_x and \vec{s}_x by α . For the inverse operation, a non-linear equation has to be solved. This can be achieved by a simple Newton iteration which converges very quickly.

In order to compute the Jacobian of the transformation f , we rotate the coordinate system of the integration over \vec{s}_x such that the z -axis is parallel to \vec{S}_x . Since only the angle θ between \vec{s}_x and \vec{S}_x is altered, the relevant integration measure is $d \cos \theta$. For the angle after the cooling $\theta' = \theta - \alpha$, we therefore have

$$d \cos \theta' = d \cos \theta \left| 1 - \frac{d\alpha}{d\theta} \right| (\cos \alpha - \cot \theta \sin \alpha) = d \cos \theta |1 - \epsilon \vec{S}_x \cdot \vec{s}_x| (\cos \alpha - \cot \theta \sin \alpha)$$

and we get for the Jacobian determinant

$$\det J_f(\vec{s}_x) = |1 - \epsilon \vec{S}_x \cdot \vec{s}_x| (\cos \alpha - \cot \theta \sin \alpha),$$

which has to be accumulated multiplicatively over all steps of the cooling/heating in order to get the aggregated value for the whole sweep.

One might expect that the optimal value of the parameter ϵ depends on the pair of temperatures. However, to keep things simple, we have used the same value of ϵ for all of them. Since β_{i+1}/β_i decreases with increasing lattice size L , also the optimal value of ϵ is decreasing with increasing L . In order to tune ϵ we have monitored the acceptance rate A . Reasonable estimates of A can already be obtained from rather short runs; Here we performed runs with 10000 cycles each. The optimal value does not depend strongly on the particular set of coupling constants.

C. Heat-bath and overrelaxation updates

In an elementary step of the algorithm, the field at a single site of the lattice is updated. Using these updates, we sweep through the lattice in typewriter fashion. To this end we use heat-bath and overrelaxation updates: In the case of the heat-bath update, we chose the component of the new field that is parallel to the nearest neighbor sum \vec{S}_x , defined in Eq. (10), as

$$s_x^{(p)} = \ln(z + (z^{-1} - z)r) / |\beta \vec{S}_x|, \quad (16)$$

where $z = \exp(-\beta |\vec{S}_x|)$ and r is a random number that is uniformly distributed in $[0, 1]$. The two orthogonal components

$$s_x^{(o,1)} = \sqrt{1 - (s_x^{(p)})^2} \sin \phi, \quad s_x^{(o,2)} = \sqrt{1 - (s_x^{(p)})^2} \cos \phi \quad (17)$$

where ϕ is uniformly distributed in $[0, 2\pi]$. In an elementary overrelaxation update the field \vec{s}_x is replaced by

$$\vec{s}'_x = 2 \frac{\vec{s}_x \cdot \vec{S}_x}{\vec{S}_x^2} \vec{S}_x - \vec{s}_x. \quad (18)$$

The overrelaxation update takes considerably less CPU-time than the heat-bath update, since it requires neither random numbers nor the evaluation of transcendental functions. The overrelaxation update by itself is not ergodic, since it keeps the energy constant. Therefore it has to be supplemented by Metropolis, or as it is the case here, heat-bath updates. It has been demonstrated that such a hybrid of heat-bath and overrelaxation updates is clearly more efficient than heat-bath updates alone. For a discussion see for example section IV of [6].

IV. NUMERICAL RESULTS

In order to test the performance of the algorithm, we have performed simulations for $L = 16, 24$ and 32 . Setting up the simulation, we closely follow Ref. [6]: In the tempering algorithm, we simulate temperatures $T = 1/\beta$ from $T_{\min} = 0.12$ up to $T_{\max} = 0.19$. The intermediate temperatures are given by

$$T_i = T_{\max} \left(\frac{T_{\min}}{T_{\max}} \right)^{(i-1)/(N_T-1)} \quad (19)$$

where $i = 1, 2, \dots, N_T$, with $N_T = 15, 27$ and 43 is used for $L = 16, 24$ and 32 , respectively. For each tempering update, we perform a heat-bath sweep followed by $\frac{5}{4}L$ overrelaxation sweeps, again as in Ref. [6]. We have not used improvements of this strategy studied in Refs. [9–11], since they are complementary to the ones discussed here. In our implementation, a heat-bath sweep takes about 5 times more CPU-time than an overrelaxation sweep. In the case of the standard tempering update the CPU-time needed is small compared with that needed for a heat-bath sweep. For the decimation, the tempering update takes a little less CPU-time than a heat-bath sweep, while for the cooling/heating method the tempering update takes about twice the CPU-time of a heat-bath sweep. In particular in the case of the cooling/heating method, we did not spend much time on optimizing our implementation. In both cases, the CPU-time taken by the tempering update is still clearly smaller than that required by the total of the heat-bath and the overrelaxation sweeps.

In the following, we will use the acceptance rate of the replica exchange step, the round trip time of the replicas and the auto-correlation time of the overlap susceptibility as figures of merit for the performance of the algorithm. Since they might depend strongly on the particular set of couplings $\{J_{ij}\}$, it is quite important to test all variants of the parallel tempering algorithm on the same sets. For each of the lattices sizes, we have therefore generated ten realizations of the $\{J_{ij}\}$, on which we performed our tests.

In the case of the standard and the decimation tempering, we have performed 100000, 200000 and 500000 update cycles for each $\{J_{ij}\}$ for $L = 16, 24$ and 32 , respectively. For the cooling/heating method we have performed 500000 update cycles throughout. These numbers are clearly larger than the number of update cycles required for equilibration. In the following, we use $\epsilon = 0.017$ for $L = 16$ and $\epsilon = 0.01$ for $L = 24$.

L	standard	decimation	cool/heat
16	0.114 — 0.122	0.237 — 0.256	0.290 — 0.249
24	0.116 — 0.126	0.239 — 0.262	0.240 — 0.320
32	0.134 — 0.145	0.262 — 0.284	

TABLE I. We give the acceptance rates for the standard and our two improved tempering methods as a function of the lattice size. The acceptance rates depend mildly on the pair of β -values of the swap. In all cases it is a monotonic function of β . In the table we give the acceptance rate for the pairs with the smallest and largest values of β .

A. Acceptance rates of the tempering method

In table I, we have summarized our results for the acceptance rates of the tempering update. We find that for the given choice of β_i , the acceptance rates can approximately be doubled by our improved tempering methods. In almost all cases, the acceptance rate slightly increases with increasing β ; only in the case of the cooling/heating method there is a decrease for $L = 16$. It seems that our choice of the parameter ϵ of the cooling/heating procedure for $L = 16$ is better suited for small values of β than for large ones. For $L = 24$, the situation is just the opposite. It seems to be beneficial, to tune ϵ for each pair of β values separately.

In the case of $L = 24$, we tried to determine by how much we can reduce N_T in the case of the improved tempering, here only considering decimation. For two of the coupling sets, we performed runs using $N_T = 22$ instead of $N_T = 27$. We find acceptance rates of $A \approx 0.146$ up to $A \approx 0.163$, i.e. still a bit larger than with the standard tempering and $N_T = 27$.

B. Round trip and autocorrelation times

Our next task is to determine, whether these increased acceptance rates lead to smaller autocorrelation times. To this end, we have studied the round trip time and the integrated auto correlation times of the overlap susceptibility at the lowest temperature $T_{\min} = 0.12$.

The round trip time is defined in the following way: we count how often a configuration runs from the highest temperature T_{\max} to the lowest temperature T_{\min} and back to T_{\max} . This is done for all $2N_T$ configurations. The round trip time t_R is then given as the number of all sweeps divided by the number of round trips.

In the case of $L = 16$, the round-trip times for the standard algorithm range from $t_R = 2495(46)$ up to $2942(53)$. These times are reduced to $t_R = 1147(12)$ up to $1467(19)$ by the decimation method. We have computed the speed-up factor $t_{R,\text{standard}}/t_{R,\text{decimation}}$ for each of the ten coupling sets. The average is 2.1. The round-trip times for the cooling/heating procedure give $t_R = 901(4)$ to $t_R = 1170(6)$, which gives comparable speed-ups of 2.6.

For $L = 24$, the round-trip times for the standard algorithm range from $t_R = 9332(209)$ up to $15485(593)$. For the decimation, we get $t_R = 4369(87)$ up to $8100(165)$. The average speed-up is 1.9. The cooling/heating gives round-trip times of $t_R = 4038(52)$ to $7437(152)$ and a speed-up of 2.0.

For $L = 32$, the round-trip times for the standard algorithm range from $t_R = 27451(374)$ up to $46206(1452)$. For the improved tempering we get $t_R = 16356(131)$ up to $27432(843)$.

L	acc. rate		round trip		$\tau_{\text{int}}(S)$	
	decim.	cool/heat	decim.	cool/heat	decim.	cool/heat
16	2.09	2.42	2.1	2.6	2.3	2.5
24	2.07	2.33	1.9	2.0	2.3	2.5
32	1.96	—	1.7	—	2.4	—

TABLE II. Speed-up for the decimation and the cooling/heating procedure with respect to the standard parallel tempering, given in terms of the acceptance rate of the exchange step, the round-trip time and the auto-correlation time of the overlap susceptibility. The error on these numbers is around 2 on the last digit.

With an average speed-up is 1.7.

The statistical errors that we quote above are only rough estimates, since they are obtained by blocking the whole data set in ten sub-ensembles. The fluctuations between different coupling sets are larger than these individual errors. Fortunately, the relative speed-ups fluctuate only mildly and can therefore be determined to about 10% accuracy.

Next we have computed integrated autocorrelation times defined by

$$\tau_{\text{int}} = \frac{1}{2} + \sum_{t=1}^{t_f} \rho(t), \quad (20)$$

where $\rho(t)$ is the normalized autocorrelation function defined by

$$\rho(t) = \frac{\langle O(i)O(i+t) \rangle - \langle O \rangle^2}{\langle O^2 \rangle - \langle O \rangle^2} \quad (21)$$

and the upper end of the summation is chosen self-consistently as $t_f = c\tau_{\text{int}}$. Since the integrated autocorrelation times of the overlap susceptibility are larger than those of the internal energy, we shall only discuss the former in the following. We have computed τ_{int} for the three choices $c = 4, 6$ and 10 . The extracted auto-correlation times differ considerably due to rather long tails in the auto-correlation functions. The variation of the integrated autocorrelation time over the different coupling sets is similar to that of the round-trip times. On the other hand, the relative speed-up in the autocorrelation times that is obtained by the improved tempering methods depends only little of the parameter c and the coupling set. In table II we give the speed-ups obtained with $c = 4$. The improvement found here is somewhat larger than that seen in the round trip times.

C. Equilibration

The equilibration time is an important quantity in spin glass simulations, because in order to perform the averages over different coupling sets, many ensembles have to be simulated, in particular since the variation of interesting observables turns out to be large. Unfortunately, we were not able to systematically study the equilibration. To get an impression, we have focussed on the coupling set 5 for $L = 16$. This coupling set has the largest round-trip time among the 10 sets that we have studied.

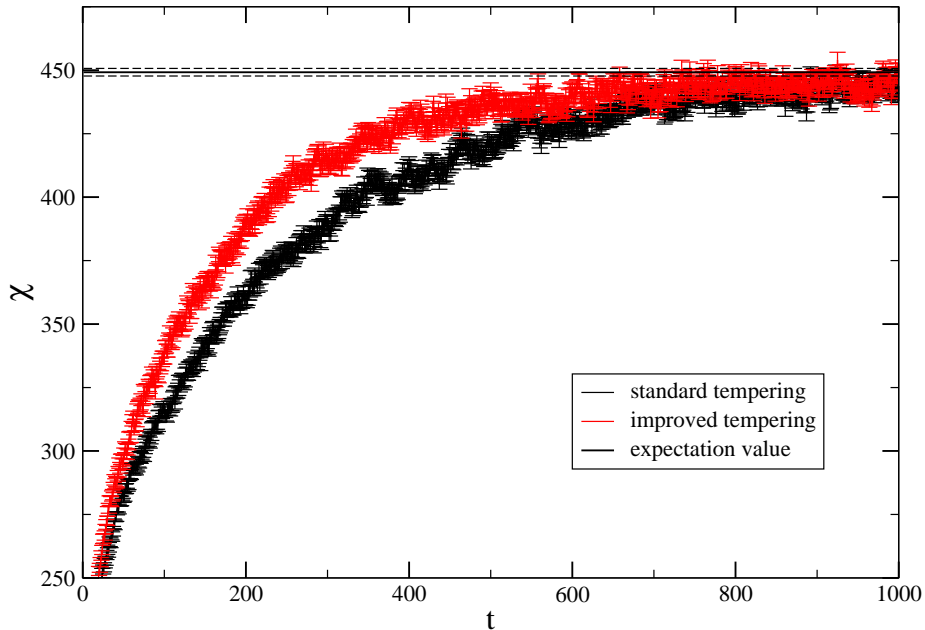


FIG. 1. (Color online) We plot the overlap susceptibility χ at $T = 0.12$ and $L = 16$ with the coupling set 5 as a function of the Monte Carlo time. We have averaged over 2000 independent runs. All runs were started with $\vec{s}_x = (1, 0, 0)$. The straight lines give our estimate for the expectation value of χ and its statistical error, obtained from the simulations discussed in the previous section. The equilibrium value is approached faster using the improved tempering than using the standard one.

We did the first 1000 iterations of the update 2000 times with different random seeds. All these 2000 simulations are started with $\vec{s}_x = (1, 0, 0)$. In figure 1 we give the averages of the overlap susceptibility for $T = 0.12$ as a function of the Monte Carlo time. We see a clear speed-up comparing the standard tempering simulation with the improved tempering one, e.g. the value 400 is reached at $t \approx 230$ in the case of the improved simulation, while in the case of the standard simulation this is the case for $t \approx 370$. These 2000 simulations did cost about 4 days of CPU time. Therefore we abstained from redoing such simulations for all our coupling sets and for larger values of L .

V. SUMMARY AND CONCLUSIONS

In this letter, we discuss two methods to improve on the replica exchange step of parallel tempering. The key idea in both is not to leave the configurations as they are and try to swap them between temperatures, but to transform them during this step. In both methods, we find an improvement of the step by roughly a factor of two.

ACKNOWLEDGMENTS

This work was supported by the DFG under the grant No HA 3150/2-1 and through the SFB/TR 9.

Appendix A: Evaluation of Eq. (14)

Here we give details of the fast numerical evaluation of $\prod_{x \in B} \sinh(R_x)$, which appears in Eq. (14). First we write

$$\prod_{x \in B} \sinh(R_x) = \exp\left(\sum_{x \in B} \ln[\sinh(R_x)]\right) \quad (\text{A1})$$

for which we need to compute $\ln[\sinh(R_x)]$ efficiently. We use

$$\ln[2 \sinh(R_x)] = R_x + \ln[1 - \exp(-2R_x)] \quad (\text{A2})$$

and proceed, depending on the value of R_x in the following way: For $R_x \gtrsim 17.5$, within the numerical precision of double precision numbers $\ln[1 - \exp(-2R_x)] = 0$. For $1 < R_x < 17.5$, we have used a pre-computed table, for $R_x = 0.9, 1.0, \dots, 17.5, 17.6$. In order to get $\ln[1 - \exp(-2R_x)]$ for any R_x in $1 < R_x < 17.5$, we have quadratically interpolated the entries of this table. We have checked that the error of this evaluation is at most of the order 10^{-16} . If $R_x < 1$, which very rarely happens in the simulation, we have used the functions of the C-library to compute $\ln[1 - \exp(-2R_x)]$.

-
- [1] C. J. Geyer in *Computer Science and Statistics: Proc. of the 23rd Symposium on the Interface*, edited by E. M. Keramidas (Interface Foundation, Fairfax Station, 1991), p. 156; K. Hukushima and K. Nemoto, *J. Phys. Soc. Jpn.* **65**, 1604 (1996); for a review, see D. J. Earl and M. W. Deem, *Phys. Chem. Chem. Phys.* **7**, 3910 (2005).
 - [2] R. H. Swendsen, J. S. Wang, *Replica Monte Carlo Simulation of Spin-Glasses*, *Phys. Rev. Lett.* **57**, 2607 (1986).
 - [3] S. B. Opper and J. Schofield, *Extended state space Monte-Carlo methods*, *Phys. Rev. E* **63**, 056701 (2001).
 - [4] A. J. Ballard and C. Jarzynski, *Replica exchange with nonequilibrium switches*, *P. Natl. Acad. Sci. USA* **106**, 12224 (2009).
 - [5] R. Alvarez Banos et al. [Janus Collaboration], *Reliable determination of the order parameter for the $D = 3$ Ising spin glass*, [arXiv:1003.2943].
 - [6] L. A. Fernandez, V. Martin-Mayor, S. Perez-Gaviro, A. Tarancon, and A. P. Young, *Phase transition in the three dimensional Heisenberg spin glass: Finite-size scaling analysis*, [arXiv:0905.0322v2], *Phys. Rev. B* **80**, 024422 (2009).
 - [7] D. X. Viet, H. Kawamura, *Monte Carlo studies of the chiral and spin orderings of the three-dimensional Heisenberg spin glass*, [arXiv:0904.3699], *Phys. Rev. B* **80**, 064418 (2009).
 - [8] M. Lüscher, *Trivializing maps, the Wilson flow and the HMC algorithm*, [arXiv:0907.5491], *Commun. Math. Phys.* **293** (2010) 899.

- [9] H. G. Katzgraber, S. Trebst, D. A. Huse, and M. Troyer, *Feedback-optimized parallel tempering Monte Carlo*, [arXiv:cond-mat/0602085], J. Stat. Mech.: Theory Exp. **2006**, P03018.
- [10] E. Bittner, A. Nussbaumer, and W. Janke, *Make life simple: unleash the full power of the parallel tempering algorithm*, [arXiv:0809.0571], Phys. Rev. Lett. **101**, 130603 (2008).
- [11] F. Hamze, N. Dickson, and K. Karimi, *Robust Parameter Selection for Parallel Tempering*, [arXiv:1004.2840], Int. J. Mod. Phys. C **21** 603 (2010).